Water Research 102 (2016) 180–189

Contents lists available at ScienceDirect

Water Research

journal homepage: www.elsevier.com/locate/watres

Nitrate and phosphate removal from agricultural subsurface drainage using laboratory woodchip bioreactors and recycled steel byproduct filters

Guanghui Hua [a, *], Morgan W. Salo [a], Christopher G. Schmit [a], Christopher H. Hay [b]

[a] Department of Civil and Environmental Engineering, South Dakota State University, Brookings, SD 57006, USA
[b] Iowa Soybean Association, 1255 SW Prairie Trail Pkwy, Ankeny, IA 50023, USA

ARTICLE INFO

Article history:
Received 20 March 2016
Received in revised form
8 June 2016
Accepted 10 June 2016
Available online 11 June 2016

Keywords:
Subsurface drainage
Nutrient removal
Nitrate
Phosphate
Woodchips bioreactors
Steel byproducts

ABSTRACT

Woodchip bioreactors have been increasingly used as an edge-of-field treatment technology to reduce the nitrate loadings to surface waters from agricultural subsurface drainage. Recent studies have shown that subsurface drainage can also contribute substantially to the loss of phosphate from agricultural soils. The objective of this study was to investigate nitrate and phosphate removal in subsurface drainage using laboratory woodchip bioreactors and recycled steel byproduct filters. The woodchip bioreactor demonstrated average nitrate removal efficiencies of 53.5–100% and removal rates of 10.1–21.6 g N/m^3/d for an influent concentration of 20 mg N/L and hydraulic retention times (HRTs) of 6–24 h. When the influent nitrate concentration increased to 50 mg N/L, the bioreactor nitrate removal efficiency and rate averaged 75% and 18.9 g N/m^3/d at an HRT of 24 h. Nitrate removal by the woodchips followed zero-order kinetics with rate constants of 1.42–1.80 mg N/L/h when nitrate was non-limiting. The steel byproduct filter effectively removed phosphate in the bioreactor effluent and the total phosphate adsorption capacity was 3.70 mg P/g under continuous flow conditions. Nitrite accumulation occurred in the woodchip bioreactor and the effluent nitrite concentrations increased with decreasing HRTs and increasing influent nitrate concentrations. The steel byproduct filter efficiently reduced the level of nitrite in the bioreactor effluent. Overall, the results of this study suggest that woodchip denitrification followed by steel byproduct filtration is an effective treatment technology for nitrate and phosphate removal in subsurface drainage.

Published by Elsevier Ltd.

1. Introduction

Agricultural subsurface drainage is a widely adopted water management practice to increase crop production in the Midwestern United States and many other areas (Fausey et al., 1995). Subsurface drainage removes excess water from the soil profile through a network of underground perforated pipes or surface ditches, which allows cultivation of agricultural fields with poor natural drainage. However, subsurface drainage systems also provide direct conduits that can transport nutrients from agricultural fields to surrounding natural water bodies (Sims et al., 1998; Jaynes et al., 2001). Elevated nutrient levels in surface waters can lead to a number of negative water quality impacts including harmful algal blooms, hypoxic zones in the ocean, and contamination of drinking water supplies (Anderson et al., 2002; Rabalais et al., 2002; Schilling, 2005).

Nitrate has been a major water quality concern for many subsurface drainage systems due to its high solubility and mobility in soils. Nitrate-nitrogen concentrations in subsurface drainage water often exceed the United States Environmental Protection Agency (USEPA) drinking water standard of 10 mg/L. Increased nitrate loading into the Mississippi River Basin from agricultural drainage in the Midwest has been identified as a major contributor to growing hypoxia in the Gulf of Mexico (Rabalais et al., 2002). Many nutrient management practices have been implemented in fields to reduce nitrate loads from subsurface drainage systems, including improved fertilizer application, controlled drainage, and denitrification bioreactors (Gilliam and Skaggs, 1986; Delgado et al., 2005; Schipper et al., 2010).

Phosphorus transport from agricultural fields to surface waters

* Corresponding author.
E-mail address: guanghui.hua@sdstate.edu (G. Hua).

http://dx.doi.org/10.1016/j.watres.2016.06.022
0043-1354/Published by Elsevier Ltd.

occurs through two primary pathways: surface runoff and subsurface drainage. Early work on agricultural phosphorus transport focused on soil erosion and surface pathways, and many studies have demonstrated that phosphorus loss occurs predominantly in surface runoff (Sharpley et al., 1993; Heathwaite and Dils, 2000). Recent studies suggest that subsurface drainage is also an important phosphorus transport pathway, and the leaching of phosphorus to subsurface drainage can be enhanced by low soil phosphorus adsorption capacity and development of preferential flows (Sims et al., 1998; Algoazany et al., 2007; Kleinman et al., 2015). Smith et al. (2015) showed that 49% of soluble phosphorus and 48% of total phosphorus losses occurred through subsurface drainage in the St. Joseph River Watershed in northeastern Indiana. King et al. (2015) demonstrated that more than 90% of all measured phosphorus concentrations in subsurface drainage of a watershed in central Ohio exceeded recommended levels (0.03 mg/L) for minimizing harmful algal blooms. It is necessary to develop practices that can control the concentrations of both nitrogen and phosphorus in subsurface drainage to protect aquatic ecosystems and public health.

Denitrification bioreactors have emerged as an important edge-of-field treatment technology to reduce nitrate loads from subsurface drainage (Blowes et al., 1994; Greenan et al., 2006; van Driel et al., 2006; Schipper et al., 2010; Christianson et al., 2011). These bioreactors typically utilize an organic carbon medium to support the growth of denitrifying bacteria which use organic electron donors to reduce nitrate to nitrogen gas (Greenan et al., 2006). Woodchips are by far the most widely used materials in field-scale denitrification bioreactors and have shown the ability to deliver long-term (>10 years) nitrate removal while requiring minimum maintenance (Blowes et al., 1994; Robertson, 2010; Christianson et al., 2011; Cooke and Bell, 2014). Under field operating conditions, woodchip bioreactors have demonstrated nitrate removal efficiencies ranging from 33 to 100%, and removal rates of 2–22 g $N/m^3/d$ (Schipper et al., 2010). Phosphorus is an essential element for the metabolism and growth of denitrifying bacteria. Hunter (2003) studied the effects of phosphate on denitrification of groundwater in sand columns and found that an N/P mass ratio of 100 or less was required to effectively reduce nitrate and prevent nitrite accumulation. The high N/P ratio suggests that a relatively small amount of phosphate is needed for the denitrifying bacteria, which agrees with the observation that wood-based bioreactors do not substantially remove phosphate (Jaynes et al., 2008). Phosphate sorption materials such as drinking water treatment residuals and biochar have been used to amend laboratory bioreactors to enhance phosphate removal (Zoski et al., 2013; Bock et al., 2015).

Emerging phosphate removal technologies are being developed to reduce phosphorus pollution using low-cost adsorption materials, such as natural minerals, synthetic filtration products, and industrial byproducts (steel slag, steel wool and turnings, fly ash, drinking water treatment residuals and others) (Penn et al., 2007; McDowell et al., 2008; Chardon et al., 2012; Erickson et al., 2012). The phosphorus adsorbents typically provide metal cations (iron, aluminum, or calcium) to bind with dissolved phosphorus to form insoluble compounds (Weng et al., 2012; Lyngsie et al., 2014). Steel chips, wools and turnings are common byproducts produced during metal processing, and they are typically recycled for steel production. These readily available steel byproducts are expected to possess high phosphate adsorption capacity due to their high iron content (Erickson et al., 2012; Weng et al., 2012). Therefore, recycled steel byproducts can be potentially used as cost-effective filtration materials to remove phosphate from subsurface drainage. Hence, we propose a two-stage treatment system using woodchip bioreactors followed by recycled steel byproduct filters to simultaneously remove nitrate and phosphate in subsurface drainage.

The objective of this study was to determine the nitrate and phosphate removal efficiency of a woodchip bioreactor followed by a steel byproduct filter in the laboratory. In this study, batch adsorption experiments were conducted to determine the phosphate adsorption capacity of selected steel chips and turnings. Column experiments were performed to evaluate the nitrate and phosphate removal by woodchips and selected steel byproducts under continuous flow conditions. The impacts of influent nutrient concentrations and hydraulic retention times on the performance of the bioreactor and the steel byproduct filter were investigated. The results of this study may lead to the development of new edge-of-field treatment systems that combine woodchip denitrification and steel byproduct filtration for nitrate and phosphate removal in subsurface drainage.

2. Materials and methods

2.1. Woodchips and steel byproducts

Table 1 summarizes the characteristics of the steel byproducts and woodchips used for this study. Four different steel byproducts were collected from a metal machining factory located in Sioux Falls, SD. Small chips, medium chips, medium turnings and large turnings were produced by processing carbon steel using different machines. After collection, steel byproducts were washed using non-phosphate soap and air dried before use. The surfaces of the steel byproduct particles were oxidized and covered with rust (iron oxides) after cleaning. All mixtures of steel byproducts and water were slightly acidic. Woodchips made from cottonwood trees were obtained from a supplier in Sioux Falls, SD. These woodchips were washed with distilled water to remove dirt and floating fine particles, and air dried before use.

2.2. Batch phosphate adsorption experiments

Batch adsorption experiments were conducted to determine the phosphate adsorption isotherm and kinetics of the steel byproducts. A temperature controlled orbital shaker (Model MaxQ 4000, Thermo Scientific, Waltham, MA) was used for the adsorption experiments. For the isotherm test, each steel byproduct (0.5–1 g) was placed in a 100 mL phosphate solution that had varying concentrations (10–40 mg P/L). The phosphate solution was prepared by dissolving $NaH_2PO_4 \cdot H_2O$ in water and the pH was adjusted to 7 using 1.0 M NaOH solution. After 24 h of adsorption at 20 °C and 100 rpm shaking, the phosphate concentration of each sample was measured. The adsorption kinetics test was also conducted at a temperature of 20 °C and 100 rpm shaking. Each steel byproduct (0.5–1 g) was placed in a 100 mL phosphate solution with an initial concentration of 30 mg P/L and a pH of 7. Samples were collected at different time intervals (0.5, 1, 2, 3, 6, and 24 h) for phosphate measurement. A Langmuir isotherm was used to model the phosphate adsorption capacity at different equilibrium concentrations. The phosphate adsorption rates were modeled using first-order reaction kinetics. These two models have been used to describe phosphate adsorption onto iron-based materials (Fu et al., 2013; Lalley et al., 2016).

2.3. Column reactor experiments

Fig. 1 shows the schematic of the two-stage upflow column reactors with the woodchips and steel byproducts. These two reactors were used for the column experiments. Both reactors were made of clear acrylic pipes and had an inside diameter of 8.7 cm. The woodchip reactor had 1.2 m of woodchips and 6 sampling

Table 1
Characteristics of steel byproducts and woodchips.

Material	Name	Type	pH[a]	Particle density[b] (g/cm^3)	Particle size[c] (distribution % by weight)
Steel byproducts[d]	Small chips	Carbon steel	6.3	5.20	0.1–2 mm (0.1–0.5 mm 55%; 0.5–1 mm 40%; 1–2 mm 5%)
	Medium chips	Carbon steel	6.2	5.50	1–10 mm (1–2 mm 18%; 2–4 mm 57%; 4–10 mm 25%)
	Medium turnings	Carbon steel	6.3	5.54	2.5–4.5 cm long, 2 mm thick
	Large turnings	Carbon steel	6.1	6.59	3–5 cm long, 5 mm thick
Woodchips	Woodchips	Cottonwood	6.8	0.63	36% large: 3–6 cm long, 0.5–2 cm wide 52% medium: 1–3 cm long, 0.5–1.5 cm wide 12% small: 0.1–1 cm long, 0.1–1 cm wide

[a] Values of pH were obtained from 1:1 by weight mixture of each material to deionized water.
[b] Particle densities were determined using the water displacement method.
[c] The particle size distributions of small and medium steel chips were obtained using the standard method for sieve analysis of particles. Particle sizes of other materials were obtained by manual separation and measurement.
[d] Steel byproducts were made from AISI 1018 carbon steel (C: 0.14–0.20%; Fe: 98.81–99.26%; Mn: 0.60–0.90%; P: ≤0.04%; S: ≤0.05%).

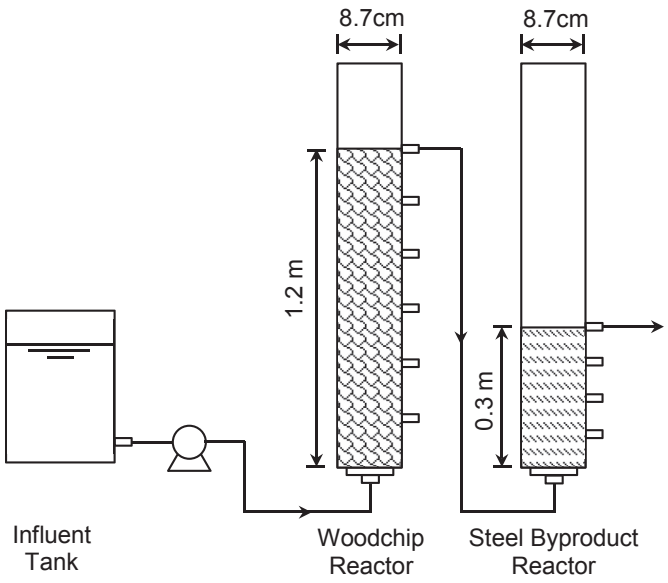

Fig. 1. Schematic of laboratory woodchip and steel byproduct reactors. (Sampling ports are evenly distributed along the height of each reactor.)

ports. Medium steel chips were selected for the column experiments based on the batch adsorption experiments. The steel byproduct reactor contained 0.3 m of steel chips and 4 sampling ports. Drainable porosity was determined by draining each reactor for 1 h, and the resulting porosities were 50% and 80% for the woodchips and steel byproducts, respectively.

The woodchip bioreactor was inoculated by a soil sample collected from an agricultural field near Brookings, SD. The soil sample (50 g) was mixed with nanopure water (4 L) and the supernatant was pumped through the woodchips at a rate of 2.5 mL/min for 5 d before the column experiments. Simulated subsurface drainage was used for the column reactor experiments, and the drainage contained typical subsurface drainage ionic constituents including Ca^{2+}, Mg^{2+}, K^{+}, Na^{+}, Cl^{-}, and SO_4^{2-} at concentrations of 5, 2.5, 2.5, 1, 15.5, and 16.7 mg/L, respectively. The selected constituent concentrations are within typical ranges in agricultural subsurface drainage (Fausey et al., 1995; Rozemeijer et al., 2010; Jia et al., 2012). In addition, trace minerals were also added to the simulated drainage including Co^{2+}, Fe^{3+}, Mn^{2+}, Mo^{7+}, Ni^{2+}, Cu^{2+}, Zn^{2+}, BO_3^{3-}, and SeO_4^{2-} at concentrations of 6.2, 52, 13.9, 2.2, 6.2, 2.6, 12, 23.4 and 18.9 μg/L, respectively. These trace minerals were added to ensure that microbial growth was not limited (Young and Tabak, 1993).

The long-term nutrient removal experiments were divided into two phases. In Phase 1, the influent nitrate and phosphate concentrations were kept at 20 mg N/L and 1 mg P/L, respectively. The influent concentrations were increased to 50 mg N/L and 10 mg P/L in Phase II as challenging conditions for the reactors. The reactors were operated continuously for 100 and 130 days under Phases I and II conditions, respectively. For both phases, the hydraulic retention time (HRT) was maintained at 24 and 9.5 h for the woodchips and steel byproducts, respectively, based on the flow rate and porosity of each material. Short-term nutrient removal experiments were also performed under Phase I nutrient concentrations to evaluate the impact of different HRTs and wet and dry cycles on the removal efficiency. During the HRT variation experiment, the HRT of the woodchips was decreased to 12 and 6 h for 10 days at each HRT. During the wet and dry cycle experiment, the two reactors were completely drained for 3 days, and the influent flow was restored for another 10 days (woodchip HRT = 24 h). This cycle was repeated twice. During the column experiments, samples were collected from different sampling ports at different time intervals for the analysis of nitrate, nitrite, phosphate, and sulfate. Table 2 presents a summary of the experimental conditions for the column reactors.

After the completion of the short and long-term column experiments, a phosphate breakthrough experiment was performed on the steel byproduct reactor to determine the total phosphate removal capacity. A 100 mg P/L solution of $NaH_2PO_4 \cdot H_2O$ (pH = 7) and three HRTs (1.2, 0.5, and 0.17 h) were used during the phosphate breakthrough experiment. The reactor was operated for 36 h at each HRT. Last, desorption experiments were conducted on the woodchips and steel byproducts to evaluate the leaching potentials of the adsorbed compounds. A 50 g sample was collected from the center of each reactor and rinsed with nanopure water three times. Then, each material was placed in 400 mL of 0.001 M KCl solution. The desorption experiment was conducted at 20 °C and 100 rpm shaking. Samples (10 mL each) were collected at time intervals of 6 h, 1 d, 3 d, 6 d, 12 d, and 20 d for the analysis of nitrate, phosphate and sulfate. After each sampling event, 10 mL of the KCl solution was added back to the desorption solution to maintain a constant water level.

2.4. Analytical methods

All solutions used in this study were prepared with ultrapure water (18 MΩ-cm) produced by a Barnstead NANOpure system. All solutions were adjusted to pH 7 using sodium hydroxide or sulfuric acid solutions. The selected neutral pH is typical of agricultural subsurface drainage (Rozemeijer et al., 2010; Jia et al., 2012). The chemicals used in this study were of American Chemical Society reagent grade and were purchased from Sigma Aldrich (St Luis, MO). Nitrate, nitrite, phosphate and sulfate were determined using

Table 2
Experimental conditions for woodchip and steel byproduct column reactors.

Column reactor	Packing density[a] (g/cm^3)	Hydraulic conductivity[b] (cm/s)	Flow rate (ml/min)	Flux rate (ml/min/cm^2)	HRT (h)
Woodchip	0.30	1.71	2.5	0.04	24
			5	0.08	12
			10	0.16	6
Steel byproduct	1.16	2.50	2.5	0.04	9.5
			5	0.08	4.8
			10	0.16	2.4

[a] Packing densities were determined by the volume occupied by the mass of each material.
[b] Hydraulic conductivities were determined by the falling-head tests at the same column packing densities.

a DX-500 ion chromatography system (Dionex, Sunnyvale, CA) equipped with a conductivity detector (CD-20, Dionex). Each sample was filtered through a 0.45 μm filter before analysis. The pH of each solution was measured with an Orion 290A+ advanced ISE/pH/mV/OPR meter (Thermo Electron, Waltham, MA).

3. Results and discussion

3.1. Phosphate adsorption isotherm and kinetics of steel byproducts

Fig. 2 shows the phosphate adsorption isotherm and kinetics of different steel byproducts. Table 3 summarizes the model parameters of the Langmuir isotherm and first-order kinetics for each material. The phosphate adsorption by steel byproducts could be described by the two models as evidenced by the high linear regression coefficients ($R^2 > 0.97$). The sizes of the steel byproducts exhibited large impacts on the phosphate adsorption capacities and rates. As shown in Fig. 2, the adsorbed phosphate per unit mass (q_e) of small and medium chips showed a sharp increase with increasing equilibrium concentrations (C_e) and reached a constant value when the C_e was higher than 1 mg P/L. When medium and large turnings were used, the q_e showed a more gradual increase with increasing C_e, and reached a constant value when the C_e was higher than 3 mg P/L. The maximum q_e values determined from the Langmuir isotherm ranged from 1.30 to 5.81 mg P/g for different steel byproducts. The phosphate adsorption capacities of these steel byproducts were similar to several other industrial byproducts that showed good phosphate removal potential, such as drinking water treatment sludge (0.89–0.95 mg P/g, Leader et al., 2008), steel slags (1.35–6.56 mg P/g, Drizo et al., 2002; McDowell et al., 2008), and iron oxide/hydroxide materials (4.43–8.21 mg P/g, Zeng et al., 2004; Fu et al., 2013; Allred and Racharaks, 2014).

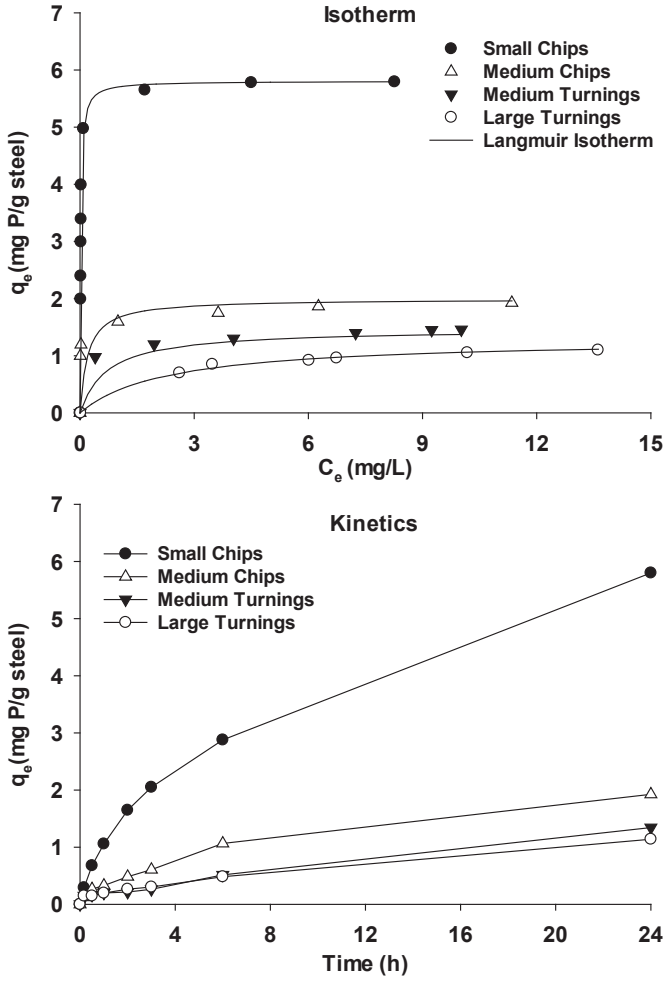

Fig. 2. Phosphate adsorption isotherm and kinetics of steel byproducts. (Experimental conditions: mass of materials = 0.5–1 g; isotherm test initial P = 10–40 mg/L; kinetics test initial P = 30 mg/L; temperature = 20 °C.)

Table 3
Phosphate adsorption isotherm and kinetics of steel byproducts.

Carbon steel[a]	Langmuir isotherm			First order kinetics	
	q_{max} (mg P/g)	k (L/mg)	R^2	k (min^{-1})	R^2
Small chips	5.81	46.5	0.999	0.276	0.978
Medium chips	2.00	5.05	0.998	0.139	0.998
Medium turnings	1.47	3.58	0.998	0.100	0.988
Large turnings	1.30	0.44	0.999	0.084	0.995

[a] Experimental conditions: temperature = 20 °C; adsorption time = 24 h; shaking = 100 rpm.

The rust on the steel particle surfaces may consist of various crystal forms including goethite (α-FeOOH), magnetite (Fe_3O_4), hematite (α-Fe_2O_3), and hydrous ferric oxide (Zeng et al., 2004; Weng et al., 2012). The mechanism of phosphate adsorption onto iron oxides is generally dominated by ligand exchange in which singly coordinated hydroxyl groups on the oxide surface are replaced by phosphate resulting in the formation of stable phosphate surface complexes (Goldberg, 1985). Also, dissolution of iron oxides can release ferrous/ferric ions which can react with phosphate to form low solubility iron-phosphate precipitates (Allred and Racharaks, 2014). Moreover, electrostatic adsorption of phosphate ions onto positively charged iron oxide surfaces may occur especially under low pH conditions (Arai and Sparks, 2007; Allred and Racharaks, 2014). In addition to the iron oxides/hydroxides, other iron-based materials such as zero-valent iron and sulfur-modified iron also exhibited high capacities for phosphate removal (McDowell et al., 2008; Allred, 2010, 2012).

Kinetic analysis of the phosphate adsorption (Table 3) showed that the rate constant (k) decreased with increasing steel particle

sizes. The phosphate removed within 6 h amounted to 50, 55, 38, and 42% of the 24 h adsorption capacities, for small chips, medium chips, medium turnings, and large turnings, respectively (Fig. 2). Leader et al. (2008) observed that iron-based drinking water residuals (0–2 mm) were able to adsorb phosphate to low levels within 4 h. Zeng et al. (2004) observed even faster phosphate adsorption kinetics using iron oxide tailing materials with an average size of 69 μm, where 64–74% of the 24 h adsorption capacity occurred within the first 0.5 h. These results suggest that particle size and other experimental conditions can have large impacts on the phosphate adsorption kinetics of iron-based materials.

The results of the batch adsorption experiments indicate that the recycled steel byproducts exhibit relatively high phosphate adsorption capacity. Although small steel chips showed the highest phosphate removal potential, these materials may be prone to clogging during field applications due to their small size. Moreover, we observed that these small chips tended to solidify to form a single mass during the experiments. Therefore, medium chips were selected for the column experiments.

3.2. Long-term nutrient removal by woodchip and steel byproduct reactors

Fig. 3 presents the long-term performance of the woodchip bioreactor and steel byproduct filter under various influent concentrations. During the 100 days of the Phase I experiments, the woodchip bioreactor consistently achieved 100% removal of nitrate, with a removal rate of 10.1 g N/m^3/d based on the reactor volume. The woodchip bioreactor did not exhibit apparent phosphate removal (<3%) during the first 7 days. The bioreactor gradually developed the capability of phosphate removal and showed steady increases in the removal with increasing operation time after 7 days. The phosphate removal efficiency increased to a maximum of 75% on the 50th day. After that, the removal efficiency moderately decreased and reached an average of 60% during the last 20 days. This result suggests that woodchips may require relatively long operating times (e.g. > 50 days) to fully develop the capability to remove phosphate. The average phosphate removal rate of the woodchips was 0.25 g P/m^3/d based on the reactor volume during Phase I experiments. The phosphate removal by the woodchip bioreactor may be explained by several mechanisms. First, the microbial growth within the bioreactor will consume certain amounts of phosphate. Second, the extracellular polymeric substances produced by the biofilm on the woodchips may adsorb phosphate (Li et al., 2015). Third, woodchips may also have the ability to adsorb phosphate from the solution. It is possible that biofilm penetration and microbial degradation of woodchips (Cameron and Schipper, 2010) may be important in developing phosphate removal capability as evidenced by the increased phosphate removal with increasing operating time. Despite the variations of phosphate in the woodchip bioreactor effluent, the steel byproduct filter completely removed the remaining phosphate (0.25–1 mg P/L) during the 100 days of operation. The average reactor volume-based phosphate removal rate of the steel byproducts was 1.0 g P/m^3/d during Phase I experiments.

During the 130 days of Phase II operation, the woodchip bioreactor achieved an average nitrate removal efficiency of 75% and an average removal rate of 18.9 g N/m^3/d, representing an 87% increase compared to Phase I conditions when influent nitrate was limiting. Both nitrate removal rates are well within the range observed in several other laboratory and field investigations (Robertson, 2010; Schipper et al., 2010; Woli et al., 2010). Steel chips showed the ability to further reduce the nitrate concentration and the removal extents varied from 2.59 to 7.10 mg N/L. Nitrate removal by the steel byproduct may be attributed to the physical and chemical adsorption onto the iron oxide surface and abiotic and biotic denitrification. The unoxidized iron surface (Fe^0) and iron corrosion

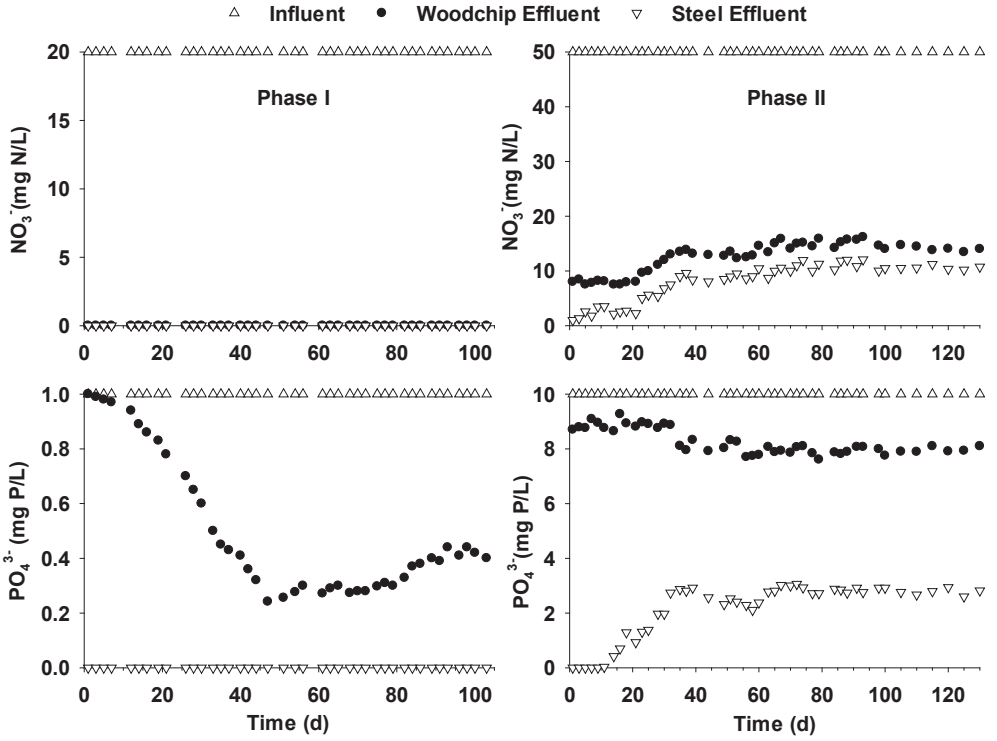

Fig. 3. Nitrate and phosphate removal by woodchip and steel byproduct reactors. (Phase I conditions: influent NO_3–N = 20 mg/L; influent PO_4^{3-}–P = 1 mg/L; woodchip HRT = 24 h; steel byproduct HRT = 9.5 h. Phase II conditions: influent NO_3–N = 50 mg/L; influent PO_4^{3-}–P = 10 mg/L; woodchip HRT = 24 h; steel byproduct HRT = 9.5 h.)

byproducts with low redox potential may reduce nitrate to nitrogen gas and ammonia through electrochemical reactions (Westerhoff and James, 2003; Allred, 2010). Similar to the Phase I operation, the phosphate removal by woodchips also increased with increasing operating time and then stabilized. The phosphate removed by the woodchips averaged 1.13 mg P/L during the first 20 days and then gradually increased to 2.01 mg P/L during the last 20 days. The average phosphate removal efficiency of the woodchips was 17.4% and the average reactor volume-based phosphate removal rate was 0.88 g P/m^3/d during Phase II experiments. This suggests that higher influent concentrations increased the phosphate removal potential of the woodchips. The steel byproduct reactor completely removed the phosphate during the initial 10 days and phosphate breakthrough occurred after that. The steel chips achieved an average reactor volume-based phosphate remove rate of 12.4 g P/m^3/d during Phase II experiments. The results in Fig. 3 suggest that the two-stage treatment system using woodchips followed by steel byproducts is an effective approach to reduce nitrate and phosphate concentrations.

3.3. Effect of HRTs on nutrient removal

Fig. 4 presents the variations of nitrate, nitrite, phosphate and sulfate at different reactor locations during the long-term performance experiments and short-term HRT variation experiments. Fig. 4a shows the average concentration profiles of the last 20 day operation under Phase I conditions. The nitrate decreased almost linearly from an initial 20 mg N/L to 3.3 mg N/L at 12 h in the woodchip bioreactor. However, it took another 12 h to completely remove nitrate. It appears that the nitrate removal kinetics by woodchips transitioned to the nitrate limiting conditions after 12 h, which necessitated long reaction times to reduce the nitrate to low levels. Christianson et al. (2011) also reported that 30–70% of nitrate was removed within 4–8 h by pilot-scale drainage bioreactors and an HRT of 10 h was necessary for 90% removal for an initial concentration of 10.1 mg N/L. Biological denitrification can be described by the Michaelis–Menten kinetics which has been used to model nitrate removal by woodchips (Ghane et al., 2015). According to this model, nitrate removal follows zero-order kinetics when the concentration is higher than the half-saturation constant (Km) and first-order kinetics when the nitrate is lower than Km. Based on the observation of nitrate variations in Fig. 4a, zero-order and first-order kinetics were used to model the first and second 12 h nitrate reductions separately. The kinetic analysis showed that nitrate removal during the first 12 h followed zero-order with a rate constant of 1.42 mg N/L/h and a R^2 value of 0.996. When the nitrate became limiting (<3.3 mg N/L) after 12 h, the nitrate removal changed to first-order kinetics with a rate constant of 0.49 h^{-1} and a R^2 value of 0.971.

Biological denitrification is a sequential reaction involving reduction of nitrate to nitrite and eventually to nitrogen gas by the enzymes nitrate reductase, nitrite reductase, and others. Nitrite is an intermediate product during denitrification. Nitrite accumulation in the woodchip bioreactor was observed during this study. Fig. 4a shows that nitrite increased near linearly from 0 to 1.60 mg N/L with increasing travel time from 0 to 12 h, which coincided with the zero-order reduction of nitrate. The accumulated nitrite accounted for 9.6% of the reduced nitrate. Nitrite quickly decreased after 12 h when nitrate became limiting and complete removal of nitrite was achieved by the woodchips at 24 h. This indicates that a 24 h HRT was necessary for the woodchips to completely remove nitrate and nitrite for an initial nitrate concentration of 20 mg N/L. Phosphate removal by woodchips primarily occurred within the first 8 h (1.00–0.50 mg P/L). Moderate reduction (0.50–0.40 mg P/L) was observed from 8 to 24 h. The

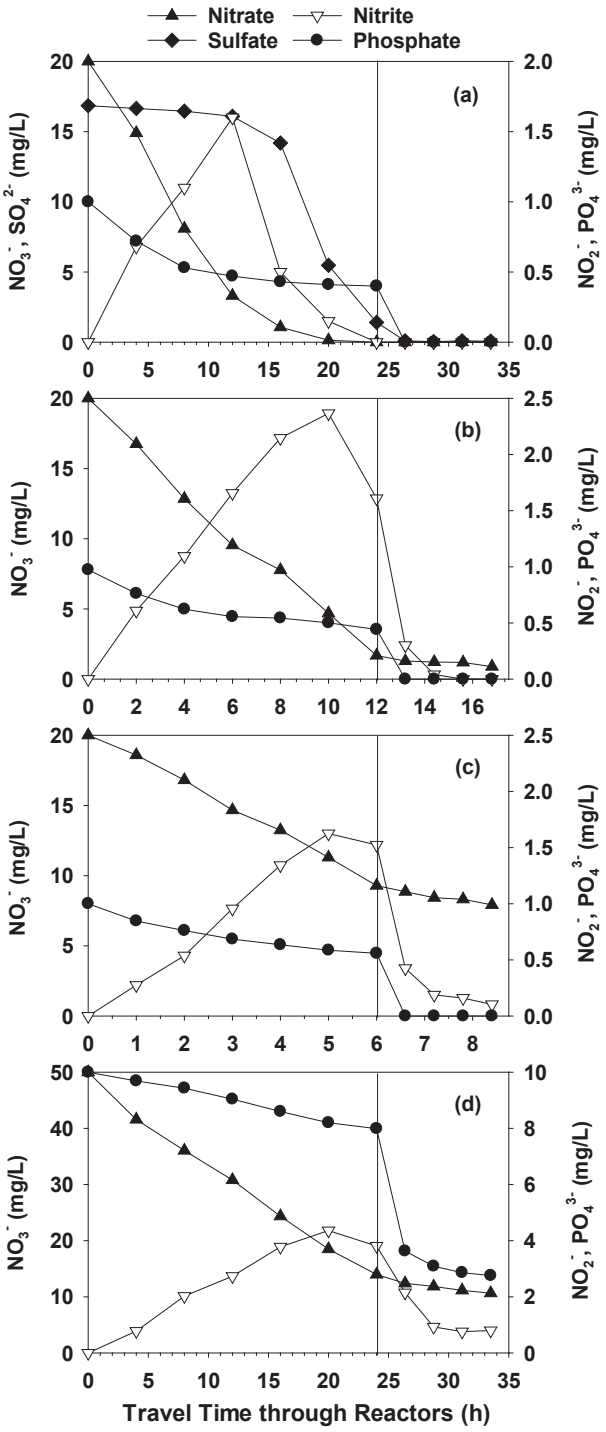

Fig. 4. Nitrate, nitrite, sulfate and phosphate profiles of woodchip and steel byproduct reactors. (Vertical lines separate woodchips and steel byproducts. (a) NO_3–N = 20 mg/L; PO_4^{3-}–P = 1 mg/L; woodchip HRT = 24 h. (b) NO_3–N = 20 mg/L; PO_4^{3-}–P = 1 mg/L; woodchip HRT = 12 h. (c) NO_3–N = 20 mg/L; PO_4^{3-}–P = 1 mg/L; woodchip HRT = 6 h. (d) NO_3–N = 50 mg/L; PO_4^{3-}–P = 10 mg/L; woodchip HRT = 24 h.)

phosphate in the woodchip effluent was quickly removed by the first 25% of the steel filter. Sulfate also declined within the woodchip reactor, but only after nitrate was depleted to less than 3.3 mg N/L. Accelerated sulfate reduction occurred when the nitrate decreased to less than 1.0 mg N/L. This indicates that nitrate at concentrations above 1 mg N/L inhibited the biological sulfate

reduction. The sulfate (1.4 mg/L) in the woodchip bioreactor effluent was quickly removed by the steel filter through adsorption and/or biological sulfate reduction.

Fig. 4b and c presents the 10 day average profiles of nitrate, nitrite and phosphate at reduced HRTs. When the woodchip bioreactor HRT was reduced to 12 and 6 h, the nitrate removal efficiency decreased to 91.5% and 53.5%, respectively. However, the reactor volume-based nitrate removal rates increased to 18.5 and 21.6 g N/m^3/d due to increased nitrate loadings. The steel byproduct filter was able to further reduce the nitrate concentrations from 1.69–9.29 mg N/L to 0.90–7.92 mg N/L at the two HRTs. Kinetic analysis suggests that nitrate removal by the woodchips followed zero-order (R^2 = 0.993–0.998), and the rate constants were 1.50 and 1.80 mg N/L/h, respectively, for 12 and 6 h HRTs. Nitrite peaked at 2.37 mg N/L (10 h) and 1.62 mg N/L (5 h), respectively, for the two HRTs. The accumulated nitrite accounted for 15.5% and 18.7% of the reduce nitrate. The woodchip bioreactor effluent had nitrite concentrations of 1.61 and 1.52 mg N/L for the two HRTs tested, which exceeded the USEPA drinking water standard of 1 mg N/L. The nitrite decreased quickly in the steel filter and reached the final concentrations of 0 and 0.10 mg N/L, respectively. Nitrite removal by the steel byproduct may be attributed to the adsorption by iron oxides and reduction by iron corrosion products to NO and N_2O (Tai and Dempsey, 2009; Dhakal et al., 2013).

When the HRT decreased to 12 h, phosphate removal by woodchips primarily occurred within the first 6 h (1–0.56 mg P/L) and reached 0.44 mg P/L in the effluent. The phosphate removal (1–0.55 mg P/L) was more evenly distributed along the woodchip reactor when the HRT was further reduced to 6 h. Therefore, the increase in HRT from 6 to 12 h had limited impact on the phosphate removal percentages by woodchips. It appears that the partition of phosphate from the solution to the woodchips became limited when the concentration was below 0.5 mg P/L. The average phosphate removal rates of the woodchips were 0.54 and 0.89 g P/m^3/d based on the reactor volume for 12 and 6 h HRTs, respectively. Despite the decrease of HRTs, the first 25% of steel filter depleted the remaining phosphate in the woodchip effluent for the two flow conditions. The steel chips achieved average phosphate removal rates of 1.79 and 4.51 g P/m^3/d based on the reactor volume for 4.8 and 2.4 h HRTs, respectively.

Fig. 4d shows the average concentration profiles of the last 20 days of operation with high influent nutrient concentrations. Nitrate exhibited a zero-order reduction (R^2 = 0.995) through woodchips with a rate constant of 1.48 mg N/L/h. Relatively high nitrite accumulation also occurred in the bioreactor which peaked at 4.36 mg N/L (13.8% of reduced nitrate) and led to an effluent concentration of 3.81 mg N/L. The phosphate decreased near linearly from 10 to 7.99 mg P/L within 24 h in the woodchip bioreactor. It is clear that high influent phosphate concentration increased phosphate removal by the woodchips. The steel byproduct reactor moderately removed nitrate from 14.0 to 10.6 mg N/L, but substantially decreased nitrite to 0.80 mg N/L (79% removal), which was below the EPA drinking water standard. Dhakal et al. (2013) also showed that magnetite removed nitrite more rapidly from solution than nitrate. Phosphate breakthrough of the entire steel byproduct reactor occurred and 65% of the woodchip effluent phosphate was removed by the steel chips.

3.4. Effect of wet and dry cycles on nutrient removal

Fig. 5 presents the impact of wet and dry cycles on the nutrient removal by the two reactors. After each 3-day dry period, the woodchip bioreactor consistently exhibited 100% removal of nitrate, suggesting that the denitrifying bacteria in the bioreactor can be reactivated quickly. Other studies reported that the

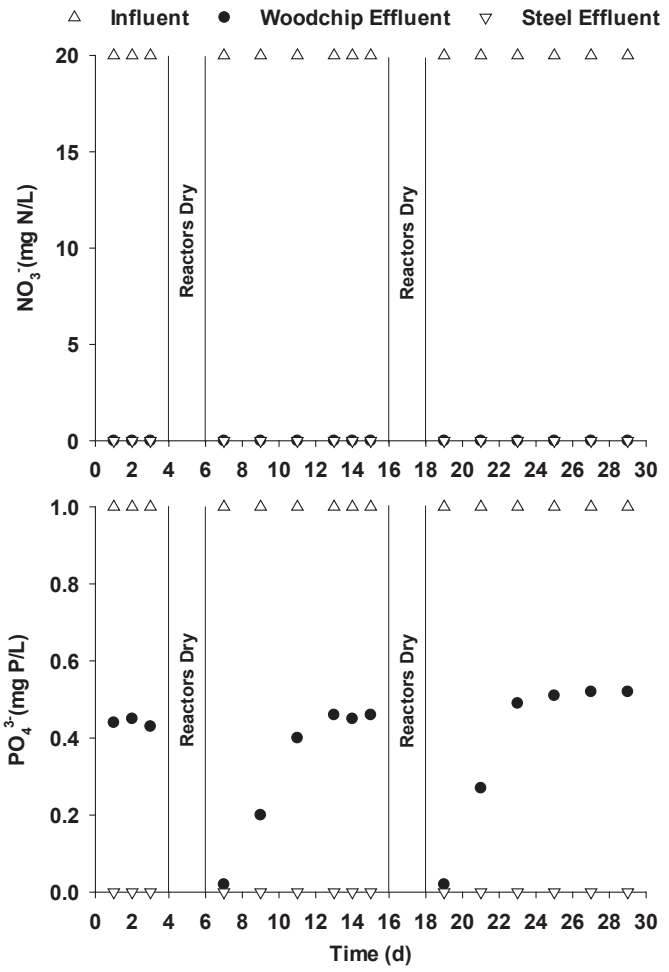

Fig. 5. Nitrate and phosphate removal by woodchip and steel byproduct reactors during wet and dry cycle experiments. (Experimental conditions: influent NO_3–N = 20 mg/L; influent PO_4^{3-}–P = 1 mg/L; woodchip HRT = 24 h; steel byproduct HRT = 9.5 h.)

denitrification performance of woodchip bioreactors was even enhanced after drying periods presumably due to the high organic carbon content in the initial flush (Woli et al., 2010). The woodchip bioreactor showed a high phosphate removal capacity during the startup of the reactor. The removal efficiency gradually declined and reached stable conditions after seven days of operation during the two cycles. This indicates that the preceding dry periods enhanced the phosphate removal capacity of the woodchips. However, this effect diminished gradually under continuous flow conditions. The steel byproduct reactor was not affected by the wet and dry cycles and completely removed the remaining phosphate in the woodchip bioreactor effluent.

3.5. Steel byproduct phosphate breakthrough experiment

Fig. 6 presents the results of the phosphate breakthrough test. The phosphate adsorption capacity of the steel filter gradually exhausted with increasing flow rates and times. Complete breakthrough of the 25% of the steel was observed at the end of 72 h. The entire steel filter showed complete breakthrough when the HRT decreased to 0.17 h. The cumulative phosphate removal through the short and long-term experiments and the breakthrough test was calculated to determine the phosphate removal capacity of the steel chips. The total mass of the phosphate removed by the medium

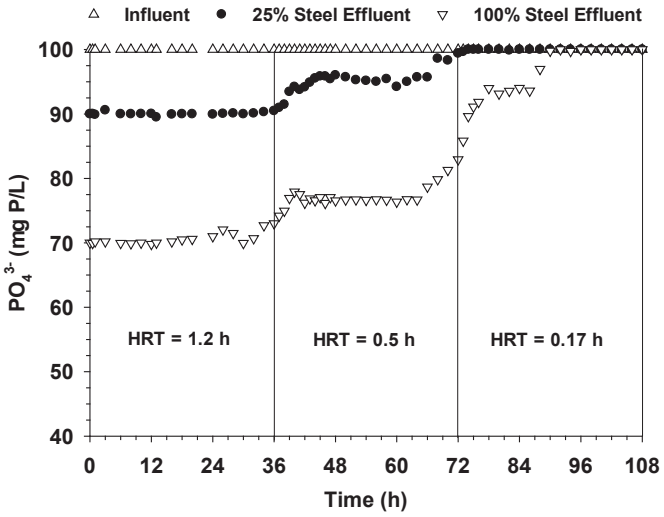

Fig. 6. Phosphate breakthrough curves of the steel byproduct reactor. (Experimental conditions: Influent PO_4^{3-}–P = 100 mg/L; HRT = 1.2, 0.5, and 0.17 h; Each HRT was operated for 36 h.)

steel chips was 2070 mg as P. The calculated phosphate adsorption capacity of this steel byproduct was 3.70 mg P/g under continuous flow conditions. This value was much higher than the capacity (2.00 mg P/g) obtained through the batch adsorption experiments. It is possible that continued rusting or corrosion of the steel chips occurred during the column experiments, which created additional sites for phosphate adsorption. The high influent concentration (100 mg P/L) used during the breakthrough test may have also contributed to the high phosphate removal capacity. Drizo et al. (2002) reported that the maximum phosphate adsorption capacity of a steel slag increased 13 times when increasing the initial phosphate concentration from 20 to 320 mg P/L. Nonetheless, both batch and column experiments suggest that recycled steel byproducts can be used as effective adsorption materials for phosphate removal in subsurface drainage. Other studies also demonstrated high phosphate adsorption capacities of iron-based materials using continuous flow column reactors (Erickson et al., 2012; Allred and Racharaks, 2014; Lyngsie et al., 2014).

3.6. Desorption of nitrate, phosphate and sulfate

Fig. 7 shows the desorption results of the woodchips and the steel chips. Nitrate in the woodchips released quickly (within 6 h) to the desorption solution and then decreased to 0 after 3 days. Phosphate and sulfate also released quickly to the solution and peaked at 1 d. After that, both compounds gradually decreased over the next 19 d. These results indicate that woodchips could recover some of the nutrients from subsurface drainage and be used as nutrient sources through land application. Sulfate desorption was observed for the steel chips and the concentration of sulfate peaked after 12 d of desorption. Steel chips did not release any phosphate or nitrate during the desorption experiments. This suggests that the binding forces (ligand exchange and precipitation) between iron oxides and phosphate are strong, and the adsorbed phosphate by the steel byproducts may have limited bioavailability.

3.7. Implications on agricultural subsurface drainage treatment

Nitrate removal kinetics is critical to the design of woodchip bioreactors. The results of this study showed that nitrate removal rate constants under non-nitrate limiting conditions varied from

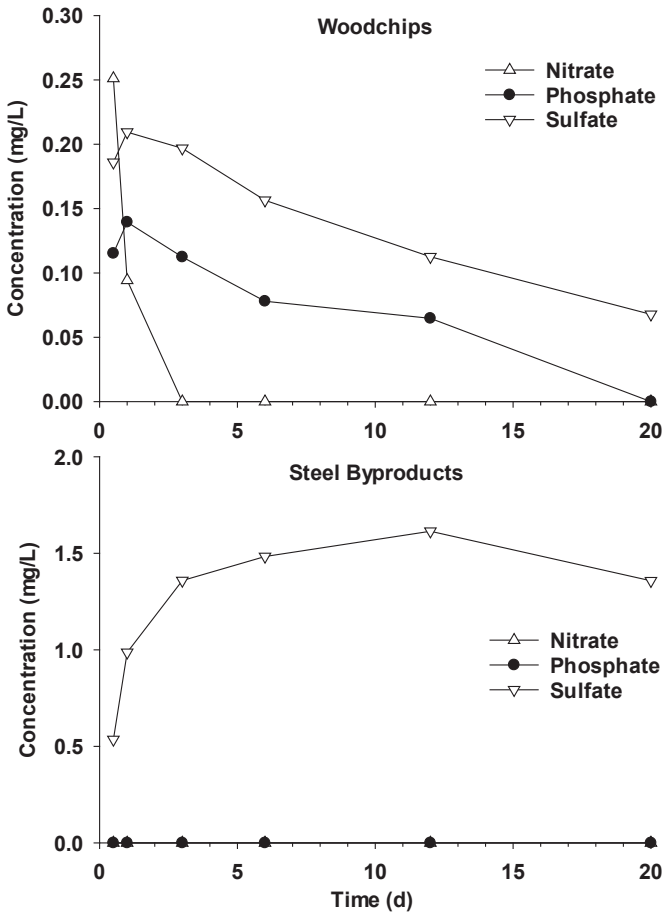

Fig. 7. Desorption of nitrate, phosphate and sulfate of woodchips and steel byproducts. (Experimental conditions: mass of material = 50 g; desorption solution = 400 mL of 0.001 M KCl; temperature = 20 °C; shaking revolution = 100 rpm.)

1.42 to 1.80 mg N/L/h for HRTs of 6–24 h and influent concentrations of 20–50 mg N/L, respectively. These rate constants are similar or higher than the nitrate removal rates obtained by other laboratory column experiments (0.38–0.97 mg N/L/h, Robertson, 2010) and field trials (0.03–1.33 mg N/L/h, Robertson, 2000). The large variations in the flow rates and concentrations in this study had limited impact on the nitrate removal rates. This result supports the notion that nitrate removal by woodchips can be operationally defined as a zero-order reaction (Schipper et al., 2010). The rate constants obtained from this study may help the design of the field woodchip denitrification bioreactors. The nitrate removal transitioned to a first-order reaction when nitrate became limiting (e.g. <3 mg N/L). Bioreactors with relatively long HRTs (>12–24 h) may be necessary to reduce the nitrate to low levels.

Nitrite accumulation was observed in the woodchip bioreactor under different experimental conditions. This raises concerns about the potential nitrite contamination from the effluent of woodchip bioreactors. Nitrite accumulation increased with decreasing HRTs and increasing nitrate concentrations. High effluent nitrite concentrations are expected under storm events with high nitrate loadings for the field bioreactors. This study showed that nitrite increased near linearly with a linear reduction of nitrate, and substantial nitrite reduction occurred only after nitrate became limiting. Relatively long HRTs (>12–24 h) would be required to effectively reduce the nitrite concentrations in the bioreactor effluent.

Field woodchip bioreactors are currently designed for 4–8 h

HRTs considering nitrate removal efficiency and economics (Christianson et al., 2011). Researchers also suggest maintaining nitrate concentration above 0.5 mg N/L in the bioreactor to avoid extreme reducing conditions which could promote sulfate reduction and methyl mercury production (Shih et al., 2011; Cooke and Bell, 2014). However, these design considerations may lead to low nitrate removal efficiency and high nitrite accumulation. High nitrate and nitrite in bioreactor effluent may negatively affect aquatic animals and drinking water supplies. The results of this study indicate that woodchip bioreactors may have to be larger (HRTs > 12–24 h) in order to effectively remove nitrate to low levels and reduce nitrite concentrations. The steel byproduct filter exhibited the ability to effectively reduce the nitrite in the woodchip bioreactor effluent in this study. Steel byproducts may also be capable of removing methyl mercury (Feyte et al., 2010), which warrants further research. Therefore, steel byproduct filters are not only highly effective at phosphate adsorption, but they can also remove multiple contaminants in subsurface drainage and reduce the undesirable consequences (nitrite accumulation and methyl mercury production) of woodchip bioreactors.

Agricultural field applications of the recycled steel byproducts for phosphate removal will depend on the drainage water flow rate and quality, phosphate adsorption capacity of the steel byproduct, cost of the material and installation, and disposal of the spent material. Algoazany et al. (2007) evaluated the phosphate transport from five subsurface drainage sites in the Little Vermillion River watershed in Illinois. The average drainage area of the five sites was 5.64 ha, and the annual average soluble phosphate mass load was 159 g P/ha/year (1994–2000). If a steel byproduct filter is designed to remove 90% of the phosphate from the above drainage conditions for five years, the estimated mass of the steel byproduct is 1090 kg, assuming a phosphate adsorption capacity of 3.70 mg P/g. The estimated filter volume is 33 ft^3 when a packing density of 1.16 g/cm^3 is used. This analysis indicates that steel byproduct filters with practical reactor sizes and material mass can be used for long-term phosphate removal in the field. Machine shop steel turnings and scraps are typically recycled at relatively low prices (e.g. $0.02–0.04/lb). These recycled steel byproducts may be available to agricultural communities at low material costs for field filter installations. After the phosphate removal capacity of the steel byproduct filter is exhausted, the spent material may be disposed of in landfills or recycled for steel production. The steel byproduct may also be regenerated by washing with an alkaline solution to recover the adsorbed phosphate (Lalley et al., 2016). The phosphate removal and recovery using the steel byproduct can be a sustainable practice for subsurface drainage phosphate management.

4. Conclusions

This study was conducted to investigate nitrate and phosphate removal in agricultural subsurface drainage using woodchip bioreactors and recycled steel byproduct filters. The results of the batch adsorption experiments showed that phosphate adsorption capacity (1.30–5.81 mg P/g) and kinetics of selected steel byproducts increased with decreasing particle sizes. During the column experiments, the woodchip bioreactor demonstrated average nitrate removal efficiencies of 53.5–100% and removal rates of 10.1–21.6 g $N/m^3/d$ for an influent concentration of 20 mg N/L and 6–24 h HRTs. When the influent nitrate concentration increased to 50 mg N/L, the nitrate removal efficiency and rate averaged 75% and 18.9 g $N/m^3/d$ at an HRT of 24 h. Nitrate removal by the woodchips followed zero-order kinetics with rate constants of 1.42–1.80 mg N/L/h when nitrate was non-limiting. Nitrite accumulation was observed in the woodchip bioreactor, and nitrite accumulation increased with decreasing HRTs from 24 to 6 h and increasing nitrate concentrations from 20 to 50 mg N/L. The accumulated nitrite amounted to 9.6–18.7% of the reduced nitrate. Substantial nitrite reduction in the woodchip bioreactor occurred only after nitrate became limiting.

Woodchips gradually developed phosphate removal capacity with increasing operating time. The woodchip bioreactor demonstrated average phosphate removal efficiencies of 17.4–56% and removal rates of 0.25–0.89 g $P/m^3/d$ for influent concentrations of 1–10 mg P/L and 6–24 h HRTs. The steel byproduct filter effectively reduced the phosphate in the woodchip reactor effluent at 2.4–9.5 h HRTs. The total phosphate adsorption capacity of the medium steel chips was 3.70 mg P/g under continuous flow conditions. Nitrite in the woodchip bioreactor effluent was effectively removed by the steel byproduct filter. Wet and dry cycles did not have negative impact on the performance of the woodchip bioreactor and the steel byproduct filter. Overall, the results of this study suggest that recycled steel byproducts can be used as effective adsorption materials for phosphate removal in subsurface drainage. The proposed two-stage treatment system using woodchip denitrification followed by steel byproduct filtration is a highly promising technology for field installations to remove nitrate and phosphate in subsurface drainage.

Acknowledgments

This research was funded by the United States Geological Survey 104b program through the South Dakota Water Resources Institute, the East Dakota Water Development District, and the Water and Environmental Engineering Research Center of South Dakota State University. The authors thank the woodchips supplier and the metal processing factory in Sioux Falls, SD for supplying the materials for this project.

References

Allred, B.J., 2010. Laboratory batch test evaluation of five filter materials for removal of nutrients and pesticides from drainage waters. Trans. ASABE 53 (1), 39–54.
Allred, B.J., 2012. Laboratory evaluation of zero valent iron and sulfur-modified iron for agricultural drainage water treatment. Groundw. Monit. Remediat. 32, 81–95.
Allred, B.J., Racharaks, R., 2014. Laboratory comparison of four iron-based filter materials for drainage water phosphate treatment. Water Environ. Res. 86, 852–862.
Algoazany, A.S., Kalita, P.K., Czapar, G.F., Mitchell, J.K., 2007. Phosphorus transport through subsurface drainage and surface runoff from a flat watershed in east central Illinois, USA. J. Environ. Qual. 36, 681–693.
Anderson, D.M., Glibert, P.M., Burkholder, J.M., 2002. Harmful algal blooms and eutrophication: nutrient sources, composition, and consequences. Estuaries 25 (4), 704–726.
Arai, Y., Sparks, D.L., 2007. Phosphate reaction dynamics in soils and soil components: a multiscale approach. Adv. Agron. 94, 135–179.
Blowes, D.W., Robertson, W.D., Ptacek, C.J., Merkley, C., 1994. Removal of agricultural nitrate from tile-drainage effluent water using in-line bioreactors. J. Contamin. Hydrol. 15, 207–221.
Bock, E., Smith, N., Rogers, M., Coleman, B., Reiter, M., Benham, B., Easton, Z.M., 2015. Enhanced nitrate and phosphate removal in a denitrifying bioreactor with biochar. J. Environ. Qual. 44, 605–613.
Cameron, S.G., Schipper, L.A., 2010. Nitrate removal and hydraulic performance of organic carbon for use in denitrification beds. Ecol. Eng. 36, 1588–1595.
Chardon, W.J., Groenenberg, J.E., Temminghoff, E.J.M., Koopmans, G.F., 2012. Use of reactive materials to bind phosphorus. J. Environ. Qual. 41, 636–646.
Christianson, L.E., Bhandari, A., Helmers, M., 2011. Pilot-scale evaluation of denitrification drainage bioreactors: reactor geometry and performance. J. Environ. Eng. 137, 213–220.
Cooke, R.A., Bell, N.L., 2014. Protocol and interactive routine for the design of subsurface bioreactors. Trans. ASABE 30 (5), 761–771.
Delgado, J.A., Khosla, R., Bausch, W.C., Westfall, D.G., Inman, D.J., 2005. Nitrogen fertilizer management based on site-specific management zones reduces potential for nitrate leaching. J. Soil Water Conserv. 60 (6), 402–410.
Dhakal, P., Matocha, C.J., Huggins, F.E., Vandiviere, M.M., 2013. Nitrite reactivity with magnetite. Environ. Sci. Tech. 47, 6206–6213.
Drizo, A., Comeau, Y., Forget, C., Chapuis, R.P., 2002. Phosphorus saturation potential: a parameter for estimating the longevity of constructed wetland systems. Environ. Sci. Tech. 36, 4642–4648.

Erickson, A.J., Gulliver, J.S., Weiss, P.T., 2012. Capturing phosphates with iron enhanced sand filtration. Water Res. 46, 3032–3042.
Fausey, N.R., Brown, L.C., Belcher, H.W., Kanwar, R.S., 1995. Drainage and water quality in Great Lakes and cornbelt states. J. Irrig. Drain. Eng. 121, 283–288.
Feyte, S., Tessier, A., Gobeil, C., Cossa, D., 2010. In situ adsorption of mercury, methylmercury and other elements by iron oxyhydroxides and organic matter in lake sediments. Appl. Geochem. 25, 984–995.
Fu, Z., Wu, F., Song, K., Lin, Y., Bai, Y., Zhu, Y., Giesy, J.P., 2013. Competitive interaction between soil-derived humic acid and phosphate on goethite. Appl. Geochem. 36, 125–131.
Ghane, E., Fausey, N.R., Brown, L.C., 2015. Modeling nitrate removal in a denitrification bed. Water Res. 71, 294–305.
Gilliam, J.W., Skaggs, R.W., 1986. Controlled agricultural drainage to maintain water quality. J. Irrig. Drain. Eng. 112, 254–263.
Goldberg, S., 1985. Chemical modeling of anion competition on goethite using the constant capacities model. Soil Sci. Soc. Am. 49, 851–856.
Greenan, C.M., Moorman, T.B., Kaspar, T.C., Parkin, T.B., Jaynes, D.B., 2006. Comparing carbon substrates for denitrification of subsurface drainage water. J. Environ. Qual. 35, 824–829.
Heathwaite, A.L., Dils, R.M., 2000. Characterising phosphorus loss in surface and subsurface hydrological pathways. Sci. Total Environ. 251–252, 523–538.
Hunter, W.J., 2003. Accumulation of nitrite in denitrifying barrier when phosphate is limiting. J. Contamin. Hydrol. 66, 79–91.
Jaynes, D.B., Colvin, T.S., Karlen, D.L., Cambardella, C.A., Meek, D.W., 2001. Nitrate loss in subsurface drainage as affected by nitrogen fertilizer rate. J. Environ. Qual. 30, 1305–1314.
Jaynes, D.B., Kaspar, T.C., Moorman, T.B., Parkin, T.B., 2008. In situ bioreactors and deep drainpipe installation to reduce nitrate loads in artificially drained fields. J. Environ. Qual. 37, 429–436.
Jia, X., DeSutter, T.M., Lin, Z., Schuh, W.M., Steele, D.D., 2012. Subsurface drainage and subirrigation effects on water quality in southeast North Dakota. Trans. ASABE 55 (5), 1757–1769.
King, K.W., Williams, M.R., Fausey, N.R., 2015. Contributions of systematic tile drainage to watershed-scale phosphorus transport. J. Environ. Qual. 44, 486–494.
Kleinman, P.J.A., Smith, D.R., Bolster, C.H., Easton, Z.M., 2015. Phosphorus fate, management, and modelling in artificially drained systems. J. Environ. Qual. 44, 460–466.
Lalley, J., Han, C., Li, X., Dionysiou, D.D., Nadagouda, M.N., 2016. Phosphate adsorption using modified iron oxide-based sorbents in lake water: kinetics, equilibrium, and column tests. Chem. Eng. J. 284, 1386–1396.
Leader, J.W., Dunne, E.J., Reddy, K.R., 2008. Phosphorus sorbing materials: sorption dynamics and physicochemical characteristics. J. Environ. Qual. 37, 174–181.
Li, W., Zhang, H., Sheng, G., Yu, H., 2015. Roles of extracellular polymeric substances in enhanced biological phosphorus removal process. Water Res. 86, 85–95.
Lyngsie, G., Borggaard, O.K., Hansen, H.C.B., 2014. A three-step test of phosphate sorption efficiency of potential agricultural drainage filter materials. Water Res. 51, 256–265.
McDowell, R.W., Sharpley, A.N., Bourke, W., 2008. Treatment of drainage water with industrial by-products to prevent phosphorus loss from tile-drained land. J. Environ. Qual. 37, 1575–1582.
Penn, C.J., Bryant, R.B., Kleinman, P.A., Allen, A.L., 2007. Removing dissolved phosphorus from ditch drainage water with phosphorus sorbing materials. J. Soil Water Conserv. 62, 269–276.
Rabalais, N.N., Turner, R.E., Dortch, Q., Justic, D., Bierman, V.J., Wiseman, W.J., 2002. Nutrient-enhanced productivity in the northern Gulf of Mexico: past, present and future. Hydrobiologia 475–476, 39–63.
Robertson, W.D., 2000. Long-term performance of in situ reactive barriers for nitrate remediation. Groundwater 38, 689–695.
Robertson, W.D., 2010. Rates of nitrate removal in woodchip media of varying age. Ecol. Eng. 36, 1581–1587.
Rozemeijer, J.C., van der Velde, Y., van Geer, F.C., Bierkens, M.F.P., Broers, H.P., 2010. Direct measurements of the tile drain and groundwater flow route contributions to surface water contamination: from field-scale concentration patterns in groundwater to catchment-scale surface water quality. Environ. Pollut. 158, 3571–3579.
Schilling, K.E., 2005. Relation of baseflow to row crop intensity in Iowa. Agric. Ecosyst. Environ. 105, 433–438.
Schipper, L.A., Robertson, W.D., Gold, A.J., Jaynes, D.B., Cameron, S.C., 2010. Denitrifying bioreactors – an approach for reducing nitrate loads to receiving waters. Ecol. Eng. 36, 1532–1543.
Sharpley, A.N., Daniel, T.C., Edwards, D.R., 1993. Phosphorus movement in the landscape. J. Prod. Agric. 6 (4), 492–500.
Shih, R., Robertson, W.D., Schiff, S.L., Ruldolph, D.L., 2011. Nitrate controls methyl mercury production in a streambed bioreactor. J. Environ. Qual. 40, 1586–1592.
Sims, J.T., Simard, R.R., Joern, B.C., 1998. Phosphorus loss in agricultural drainage: historical perspective and current research. J. Environ. Qual. 27, 277–293.
Smith, D.R., King, K.W., Johnson, L., Francesconi, W., Richards, P., Baker, D., Sharpley, A.N., 2015. Surface runoff and tile drainage transport of phosphorus in the Midwestern United States. J. Environ. Qual. 44, 495–502.
Tai, Y., Dempsey, B.A., 2009. Nitrite reduction with hydrous ferric oxide and Fe(II): stoichiometry, rate, and mechanism. Water Res. 43, 546–552.
van Driel, P.W., Robertson, W.D., Merkley, L.C., 2006. Denitrification of agricultural drainage using wood-based reactors. Trans. ASABE 49 (2), 565–573.
Weng, L., Riemsdijk, W.H.V., Hiemstra, T., 2012. Factors controlling phosphate interaction with iron oxides. J. Environ. Qual. 41, 628–635.
Westerhoff, P., James, J., 2003. Nitrate removal in zero-valent iron packed columns. Water Res. 37, 1818–1830.
Woli, K.P., David, M.B., Cooke, R.A., McIsaac, G.R., Mitchell, C.A., 2010. Nitrogen balance in and export in and export from agricultural fields associated with controlled drainage systems and denitrifying bioreactors. Ecol. Eng. 36, 1558–1566.
Young, J.C., Tabak, H.H., 1993. Multilevel protocol for assessing the fate and effect of toxic organic chemicals in anaerobic treatment processes. Water Environ. Res. 65, 34–45.
Zeng, L., Li, X., Liu, J., 2004. Adsorptive removal of phosphate from aqueous solutions using iron oxide tailings. Water Res. 38, 1318–1326.
Zoski, E.D., Lapen, D.R., Gottschall, N., Murrell, R.S., Schuba, B., 2013. Nitrogen, phosphorus, and bacteria removal in laboratory-scale woodchip bioreactors amended with drinking water treatment residuals. Trans. ASABE 56 (4), 1339–1347.